FINITE DIFFERENCE SOLUTION FOR BIOPOTENTIALS OF AXIALLY SYMMETRIC CELLS

MAURICE KLEE *and* ROBERT PLONSEY

From the Department of Biomedical Engineering, Case Western Reserve University, Cleveland, Ohio 44106. Dr. Klee's present address is the Mathematical Research Branch, National Institute of Arthritis, Metabolic and Digestive Diseases, National Institutes of Health, Bethesda, Maryland 20014.

ABSTRACT The finite difference equations necessary for calculating the three-dimensional, time-varying biopotentials within and surrounding axially symmetric cells are presented. The method of sucessive overrelaxation is employed to solve these equations and is shown to be rapidly convergent and accurate for the exemplary problem of a spheroidal cell under uniform field stimulation.

In order to understand the electrical behavior of biological tissue, analytic solutions have been developed for the three-dimensional biopotentials within and surrounding spherical and cylindrical cells (Clark and Plonsey, 1968; Eisenberg and Engle, 1970; Eisenberg and Johnson, 1970; Hellerstein, 1968; Lorente de Nó, 1947; Rall, 1969; Vayo, 1965; Weinberg, 1942). Further development of analytic solutions for more complicated cell shapes has been limited by the nonclassical boundary conditions at biological membranes. In this paper, a finite difference numerical technique is presented which handles the biological boundary conditions and accepts all cell shapes which have axial symmetry.

INTRODUCTION

Biopotentials are solutions to Poisson's partial differential equation subject to the boundary conditions at biological membranes and subject to a condition at infinity (Plonsey and Heppner, 1967). A finite difference numerical solution for these biopotentials consists of three parts: choosing a set of points within the space of interest, writing finite difference equations for the potential at each of these points, and solving the resulting set of simultaneous equations.

The choice of point location is determined by the particular biological system under study. For example, Fig. 1 illustrates three representative ways of choosing sets of points for spheroidal-shaped cells subjected to uniform field stimulation along their axis of symmetry. Points were placed in only one quadrant of a plane con-

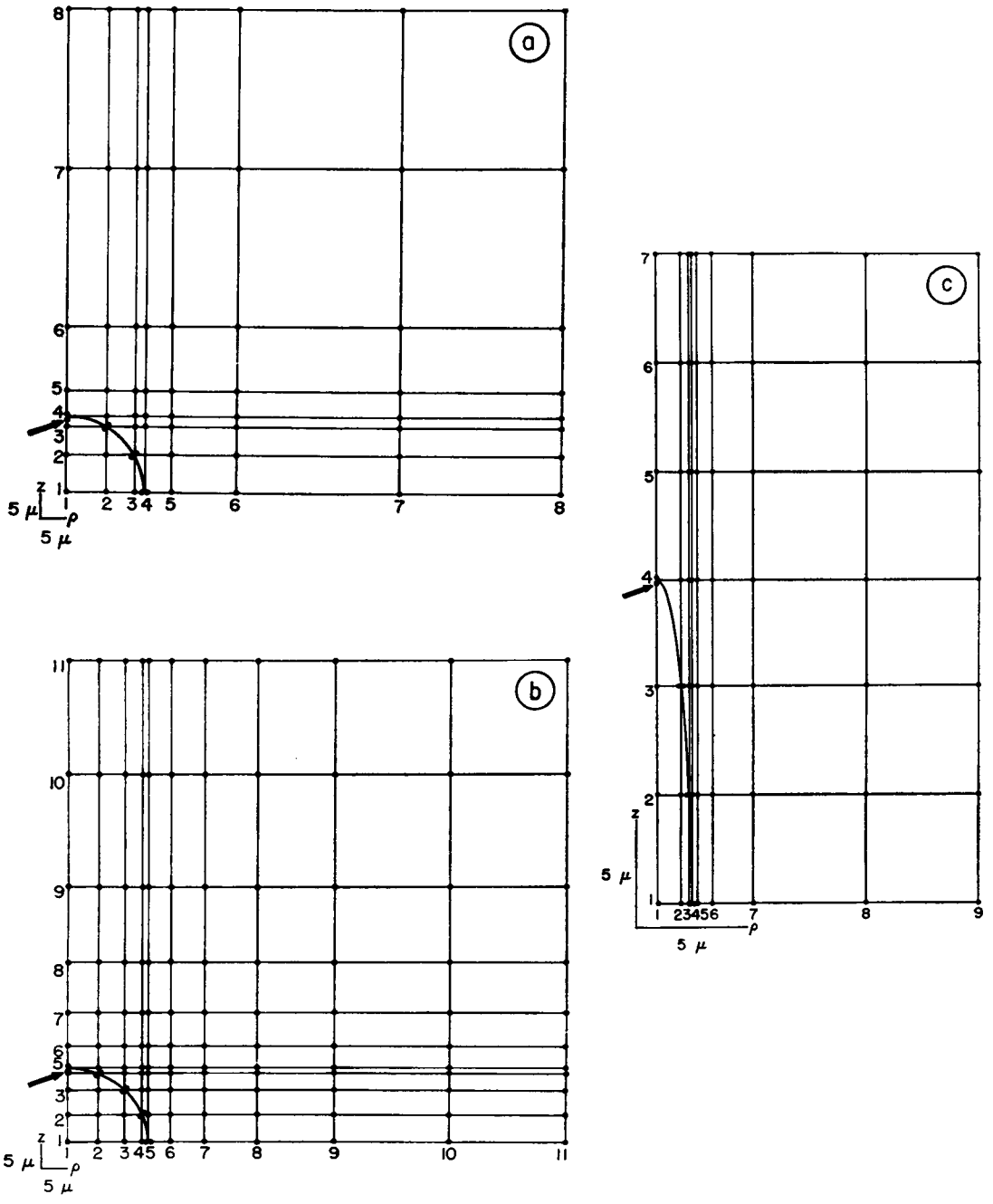

FIGURE 1 Mesh plots for spheroidal cells. (*a*) Sphere, 15 μ radius, 68 mesh points. (*b*) Sphere, 15 μ radius, 126 mesh points. (*c*) Prolate spheroid, 15 μ major axis, 1.5 μ minor axis, 67 mesh points. Arrows indicate points used for Figs. 5 and 6.

taining the center of the spheroid and parallel to the applied field, since the potentials in the rest of space are related to these potentials by symmetry. The nonuniform spacing between the mesh points results from requiring equal spacing between points lying on the cell membrane.

Once the choice of points has been made, finite difference equations for the potential at each point are written as a linear weighted average of the potentials at surrounding points. The particular equation used at any given point is determined by the location of that point: if the point lies in the intra- or extracellular space, an equation approximating Poisson's equation is used; if the point lies on a biological membrane, an equation approximating the boundary conditions at a biological membrane is used; and, if the point lies at the edge of the space of interest, an equation approximating the condition at infinity is used. These equations will be discussed in the first section of this paper.

Once these equations have been written, the solution for the biopotentials is obtained as the set of potential values which will simultaneously satisfy all of these equations. Either the direct method of gaussian elimination (Isaacson and Keller, 1966) or, preferably, the iterative method of successive overrelaxation (Forsythe and Wasow, 1960; Kinnen and Newton, 1966; Terry, 1967) can be used to find this set of potential values. This latter method, as applied to the calculation of biopotentials, will be discussed in the last section of this paper.

With this overview in mind, we will now proceed to discuss the three types of finite difference equations needed for the calculation of biopotentials and the use of successive overrelaxation in solving these equations.

FINITE DIFFERENCE EQUATIONS

Poisson's Equation

The electrical parameters characteristic of a biological medium allow us to use Poisson's equation at all points distant from a biological membrane (Plonsey and Heppner, 1967). Finite computer storage restricts us to axially symmetric boundaries and sources, whereby a three-dimensional problem can be described by only two dimensions, thus producing a savings of $n^3 - n^2$ storage spaces, where n is the number of mesh points along a coordinate axis. Poisson's equation in cylindrical coordinates under this assumption of axial symmetry becomes:

$$\frac{\partial^2\Phi(\rho, z, t)}{\partial\rho^2} + \frac{1}{\rho}\frac{\partial\Phi(\rho, z, t)}{\partial\rho} + \frac{\partial^2\Phi(\rho, z, t)}{\partial z^2} = -\frac{I(\rho, z, t)_{\text{applied}}}{\sigma},$$

where $\Phi(\rho, z, t)$ is the unknown potential function, $I(\rho, z, t)_{\text{applied}}$ is the applied volume source density (amperes per cubic centimeter), σ is the conductivity of the medium at the *source* (reciprocal ohms per centimeter), z is measured along the axis of symmetry, ρ is the radial coordinate, and t is time.

The time variation is best handled by assuming a sinusoidal source and using com-

plex phasor notation. The response of the system to other time variations can be synthesized by the weighted linear superposition of sinusoids of various frequencies. In complex phasor notation, Poisson's equation becomes:

$$\frac{\partial^2\hat{\Phi}(\rho, z)e^{j\omega t}}{\partial\rho^2} + \frac{1}{\rho}\frac{\partial\hat{\Phi}(\rho, z)e^{j\omega t}}{\partial\rho} + \frac{\partial^2\hat{\Phi}(\rho, z)e^{j\omega t}}{\partial z^2} = -\frac{\hat{I}(\rho, z)_{\text{applied}}e^{j\omega t}}{\sigma},$$

where ω is the angular frequency of the source, the circumflex indicates a complex quantity, and $j = \sqrt{-1}$. Physical values are obtained by taking either the real or imaginary part of the complex quantities $\hat{I}(\rho, z)_{\text{applied}}e^{j\omega t}$ and $\hat{\Phi}(\rho, z)e^{j\omega t}$. During calculations, the $e^{j\omega t}$ is suppressed, giving us the complex Poisson's equation:

$$\frac{\partial^2\hat{\Phi}(\rho, z)}{\partial\rho^2} + \frac{1}{\rho}\frac{\partial\hat{\Phi}(\rho, z)}{\partial\rho} + \frac{\partial^2\hat{\Phi}(\rho, z)}{\partial z^2} = -\frac{\hat{I}(\rho, z)_{\text{applied}}}{\sigma}. \tag{1}$$

In displaying complex quantities, it is useful to employ the identity:

$$\text{real } (\hat{x}) + j\,\text{imag } (\hat{x}) = |\hat{x}|e^{j\theta},$$

where

$$|\hat{x}| = +\sqrt{[\text{real } (\hat{x})]^2 + [\text{imag } (\hat{x})]^2},$$

and

$$\theta = \tan^{-1}[\text{imag } (\hat{x})/\text{real } (\hat{x})].$$

The applied source is best handled by assuming that the unknown potential is made up of two parts, one due to the source and one induced by the biological boundaries, that is:

$$\hat{\Phi}(\rho, z) = \hat{\Phi}(\rho, z)_{\text{applied}} + \hat{\Phi}(\rho, z)_{\text{induced}},$$

where

$$\nabla^2\hat{\Phi}(\rho, z)_{\text{applied}} = -\frac{\hat{I}(\rho, z)_{\text{applied}}}{\sigma}.$$

Substituting these equations into equation 1, we are left with Laplace's equation for the induced potential, that is:

$$\frac{\partial^2\hat{\Phi}(\rho, z)_{\text{induced}}}{\partial\rho^2} + \frac{1}{\rho}\frac{\partial\hat{\Phi}(\rho, z)_{\text{induced}}}{\partial\rho} + \frac{\partial^2\hat{\Phi}(\rho, z)_{\text{induced}}}{\partial z^2} = 0. \tag{2}$$

This equation is easier to handle than equation 1 and we can easily regain the total potential by adding the known applied potential to the solution for the induced potential.

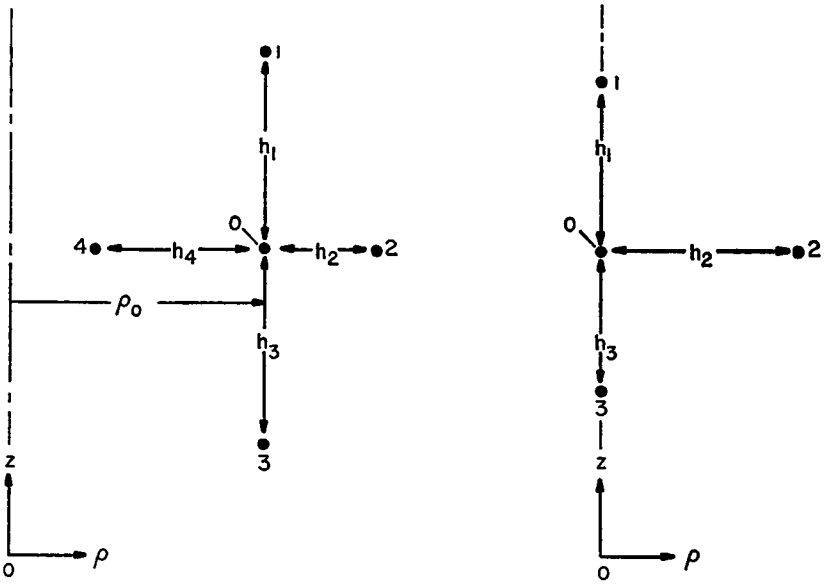

FIGURE 2 Mesh point arrangement for Poisson's equation. (*a*) Center point 0 off axis of symmetry. (*b*) Center point 0 on axis of symmetry.

Second order, finite difference approximations to equation 2 are commonly available (Greenspan, 1965; Shortley et al., 1947). In five-point form, with non-uniform mesh spacing and with reference to Fig. 2 *a*, we can write the following equation for the potential at mesh point 0 when 0 is not on the axis of symmetry:

$$\begin{aligned}\Phi_{\text{induced (0)}} = \{&[2\rho_0/(h_1[h_1 + h_3])]\Phi_{\text{induced (1)}} + [2\rho_0/(h_3[h_1 + h_3])]\Phi_{\text{induced (3)}} \\ &+ [(2\rho_0 + h_4)/(h_2[h_4 + h_2])]\Phi_{\text{induced (2)}} \\ &+ [(2\rho_0 - h_2)/(h_4[h_4 + h_2])]\Phi_{\text{induced (4)}}\} \\ &/\{2\rho_0/(h_1h_3) + (2\rho_0 + h_4 - h_2)/(h_4h_2)\}, \qquad (3)\end{aligned}$$

where ρ_0 is the radial distance to point 0. When point 0 is on the axis of symmetry, the following equation, obtained by applying axial symmetry to the finite difference, rectangular Laplace equation, is used (see Fig. 2 *b*):

$$\begin{aligned}&\Phi_{\text{induced (0)}} \\ &= \{[h_2^2/(h_1[h_1 + h_3])]\Phi_{\text{induced (1)}} + [h_2^2/(h_3[h_1 + h_3])]\Phi_{\text{induced (3)}} + 2\Phi_{\text{induced (2)}}\} \\ &\qquad /\{2 + h_2^2/(h_1h_3)\}. \qquad (4)\end{aligned}$$

These two equations (3 and 4) constitute the finite difference expressions for Poisson's equation and thus hold at all mesh points not on a biological membrane or used to satisfy the condition at infinity.

Boundary Conditions at a Biological Membrane

The boundary conditions at a biological membrane are non classical in that both the potential and, in general, its normal derivative are discontinuous. Mathematically, under the assumed sinusoidal conditions, these boundary conditions are written (Plonsey, 1969, equations 5.160 and 5.161):

$$-\sigma_{\text{intra}} \frac{\partial \hat{\Phi}_{\text{intra}}}{\partial n} = -\sigma_{\text{extra}} \frac{\partial \hat{\Phi}_{\text{extra}}}{\partial n} = \hat{J}_{\text{memb}}, \quad (5)$$

$$(\sigma_{\text{memb}} + j\omega C_{\text{memb}})(\hat{\Phi}_{\text{intra}} - \hat{\Phi}_{\text{extra}}) = \hat{Y}_{\text{memb}}(\hat{\Phi}_{\text{intra}} - \hat{\Phi}_{\text{extra}}) = \hat{J}_{\text{memb}}, \quad (6)$$

where $\hat{\Phi}_{\text{intra}}$ and $\hat{\Phi}_{\text{extra}}$ are, respectively, the total (applied plus induced) intra- and extracellular potentials, n is the axially symmetric outward normal at the membrane surface, $\hat{J}_{\text{memb}}$ is the normal current per unit area crossing the membrane, σ_{intra} and σ_{extra} are, respectively, the intra- and extracellular conductivities in reciprocal ohms per centimeter, σ_{memb} is the membrane conductivity in reciprocal ohms per square centimeter, C_{memb} is the membrane capacitance in farads per square centimeter, and $\hat{Y}_{\text{memb}} = \sigma_{\text{memb}} + j\omega C_{\text{memb}}$ is the complex membrane admittance in reciprocal ohms per square centimeter. The first of these equations expresses the requirement that the normal current density be continuous across the thin membrane while the second equation relates this current density to the resulting transmembrane potential produced by the admittance of the membrane under the assumed passive conditions.

To change these differential equations into finite difference equations one must first consider each mesh point which lies on the membrane as a double point, with one point just inside and one point just outside the boundary (see Fig. 3). One then rearranges the boundary condition equations so that the coupling between the inside and outside is only through the potential and not through its derivative, that is, equations 5 and 6 are rewritten as follows:

$$\hat{Y}_{\text{memb}} \hat{\Phi}_{\text{intra}} + \sigma_{\text{intra}} \frac{\partial \hat{\Phi}_{\text{intra}}}{\partial n} = \hat{Y}_{\text{memb}} \hat{\Phi}_{\text{extra}},$$

$$\hat{Y}_{\text{memb}} \hat{\Phi}_{\text{extra}} - \sigma_{\text{extra}} \frac{\partial \hat{\Phi}_{\text{extra}}}{\partial n} = \hat{Y}_{\text{memb}} \hat{\Phi}_{\text{intra}}.$$

Using the separation of induced and applied potential, introduced in the discussion of Poisson's equation, these expressions become:

$$\hat{Y}_{\text{memb}} \hat{\Phi}_{\substack{\text{induced} \\ \text{intra}}} + \sigma_{\text{intra}} \frac{\partial \hat{\Phi}_{\substack{\text{induced} \\ \text{intra}}}}{\partial n} - \sigma_{\text{intra}} \hat{E}_{\substack{\text{applied} \\ \text{normal}}} \Big|_{\text{memb}} = \hat{Y}_{\text{memb}} \hat{\Phi}_{\substack{\text{induced} \\ \text{extra}}}, \quad (7)$$

$$\hat{Y}_{\text{memb}} \hat{\Phi}_{\substack{\text{induced} \\ \text{extra}}} - \sigma_{\text{extra}} \frac{\partial \hat{\Phi}_{\substack{\text{induced} \\ \text{extra}}}}{\partial n} + \sigma_{\text{extra}} \hat{E}_{\substack{\text{applied} \\ \text{normal}}} \Big|_{\text{memb}} = \hat{Y}_{\text{memb}} \hat{\Phi}_{\substack{\text{induced} \\ \text{intra}}}, \quad (8)$$

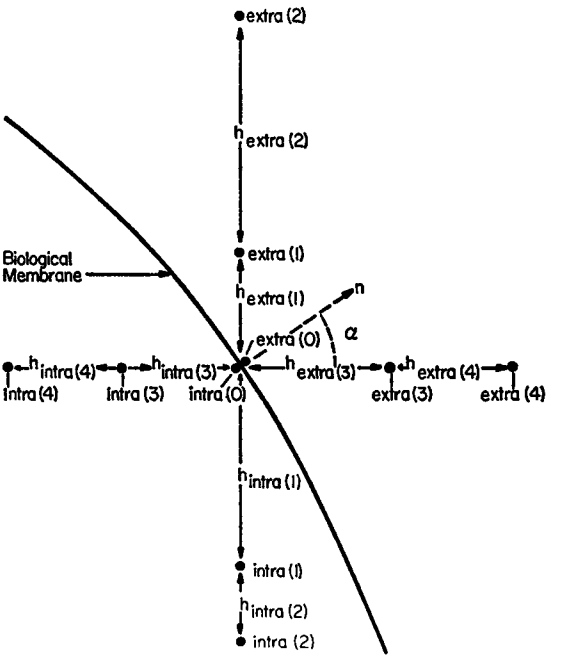

FIGURE 3 Mesh point arrangement at a biological membrane. n is the axially symmetric outward normal at the membrane surface where a double set of points have been defined.

where

$$\hat{E}_{\substack{\text{applied}\\\text{normal}}}\Big|_{\text{memb}} = -\nabla\hat{\Phi}(\rho, z)_{\text{applied}} \cdot \vec{\mathbf{n}}$$

is the known normal component of applied electric field evaluated at the membrane surface. Now, following Greenspan's method for obtaining a third-order finite difference approximation to the normal derivative (Greenspan, 1965, pp. 39–42), but with the mesh points of Fig. 3, we can write the following:

$$\frac{\partial\hat{\Phi}_{\substack{\text{induced}\\\text{intra}}}}{\partial n}\Bigg|_{\text{intra}(0)} = \sum_{i=0}^{4} a_{\text{intra}(i)}\,\hat{\Phi}_{\substack{\text{induced}\\\text{intra}(i)}}, \tag{9}$$

$$\frac{\partial\hat{\Phi}_{\substack{\text{induced}\\\text{extra}}}}{\partial n}\Bigg|_{\text{extra}(0)} = \sum_{i=0}^{4} a_{\text{extra}(i)}\,\hat{\Phi}_{\substack{\text{induced}\\\text{extra}(i)}}, \tag{10}$$

where (see Fig. 3):

$$a_{\text{intra (1)}} = -[(h_{\text{intra (1)}} + h_{\text{intra (2)}})/(h_{\text{intra (1)}}h_{\text{intra (2)}})] \sin\alpha,$$

$$a_{\text{extra (1)}} = [(h_{\text{extra (1)}} + h_{\text{extra (2)}})/(h_{\text{extra (1)}}h_{\text{extra (2)}})] \sin\alpha,$$

$$a_{\text{intra (2)}} = [h_{\text{intra (1)}}/(h_{\text{intra (2)}}(h_{\text{intra (1)}} + h_{\text{intra (2)}}))] \sin\alpha,$$

$$a_{\text{extra (2)}} = -[h_{\text{extra (1)}}/(h_{\text{extra (2)}}(h_{\text{extra (1)}} + h_{\text{extra (2)}}))] \sin \alpha,$$

$$a_{\text{intra (3)}} = -[(h_{\text{intra (3)}} + h_{\text{intra (4)}})/(h_{\text{intra (3)}}h_{\text{intra (4)}})] \cos \alpha,$$

$$a_{\text{extra (3)}} = [(h_{\text{extra (3)}} + h_{\text{extra (4)}})/(h_{\text{extra (3)}}h_{\text{extra (4)}})] \cos \alpha,$$

$$a_{\text{intra (4)}} = [h_{\text{intra (3)}}/(h_{\text{intra (4)}}(h_{\text{intra (3)}} + h_{\text{intra (4)}}))] \cos \alpha,$$

$$a_{\text{extra (4)}} = -[h_{\text{extra (3)}}/(h_{\text{extra (4)}}(h_{\text{extra (3)}} + h_{\text{extra (4)}}))] \cos \alpha,$$

$$a_{\text{intra (0)}} = -[a_{\text{intra (1)}} + a_{\text{intra (2)}} + a_{\text{intra (3)}} + a_{\text{intra (4)}}],$$

$$a_{\text{extra (0)}} = -[a_{\text{extra (1)}} + a_{\text{extra (2)}} + a_{\text{extra (3)}} + a_{\text{extra (4)}}].$$

Substituting equations 9 and 10 into equations 7 and 8 and rearranging, we arrive at the following finite difference equations for the induced potentials at points intra (0) and extra (0):

$$\hat{\Phi}_{\substack{\text{induced} \\ \text{intra(0)}}} = \{\hat{\Phi}_{\substack{\text{induced} \\ \text{extra(0)}}} - (\sigma_{\text{intra}}/\hat{Y}_{\text{memb}}) \left(-\hat{E}_{\substack{\text{applied} \\ \text{normal}}}\right|_0 + \sum_{i=1}^{4} a_{\text{intra}(i)} \hat{\Phi}_{\substack{\text{induced} \\ \text{intra}(i)}})\}/\{1 + (\sigma_{\text{intra}}/\hat{Y}_{\text{memb}})a_{\text{intra(0)}}\}, \quad (11)$$

$$\hat{\Phi}_{\substack{\text{induced} \\ \text{extra(0)}}} = \{\hat{\Phi}_{\substack{\text{induced} \\ \text{intra(0)}}} + (\sigma_{\text{extra}}/\hat{Y}_{\text{memb}}) \left(-\hat{E}_{\substack{\text{applied} \\ \text{normal}}}\right|_0 + \sum_{i=1}^{4} a_{\text{extra}(i)} \hat{\Phi}_{\substack{\text{induced} \\ \text{extra}(i)}})\}/\{1 - (\sigma_{\text{extra}}/\hat{Y}_{\text{memb}})a_{\text{extra(0)}}\}. \quad (12)$$

For membrane points adjacent to the z axis, equation 11 is modified slightly by symmetry considerations. Specifically, $\hat{\Phi}_{\substack{\text{induced} \\ \text{intra(4)}}}$ is set equal to $\hat{\Phi}_{\substack{\text{induced} \\ \text{intra(0)}}}$ and equation 11 is rearranged as follows:

$$\hat{\Phi}_{\substack{\text{induced} \\ \text{intra(0)}}} = \{\hat{\Phi}_{\substack{\text{induced} \\ \text{extra(0)}}} - (\sigma_{\text{intra}}/\hat{Y}_{\text{memb}}) \left(-\hat{E}_{\substack{\text{applied} \\ \text{normal}}}\right|_0 + \sum_{i=1}^{3} a_{\text{intra}(i)} \hat{\Phi}_{\substack{\text{induced} \\ \text{intra}(i)}})\}/\{1 + (\sigma_{\text{intra}}/\hat{Y}_{\text{memb}})(a_{\text{intra(0)}} + a_{\text{intra(4)}})\}. \quad (13)$$

For points on the z axis, the symmetry is automatically included by cos α becoming zero, thus setting $a_{\text{intra (3)}} = a_{\text{intra (4)}} = a_{\text{extra (3)}} = a_{\text{extra (4)}} = 0$.

These sets of two equations (11 and 12, or 13 and 12) constitute the finite difference expressions for the boundary conditions at a biological membrane, where a double set of mesh points must be defined to handle the discontinuity in potential.

Condition at Infinity

The condition at infinity for cells embedded in a large mass of tissue is that the induced potential, introduced in the discussion of Poisson's equation, must go to zero as one approaches infinity. To satisfy this condition a trial and error procedure must be employed in which the number of mesh points and/or the mesh spacing is increased until the calculated potentials at the edges of the mesh are sufficiently small.

In terms of finite difference equations, this empirical procedure becomes a set of equations for the potentials at the outermost tier of mesh points and a set of conditions for the potentials calculated, using the finite difference approximations to Laplace's equation, at the next inner tier of points. At the outermost mesh points we write:

$$\hat{\Phi}_{\substack{\text{induced}\\\text{extra}}}\Big|_{\substack{\text{outermost}\\\text{tier}}} = 0. \tag{14}$$

We then adjust the mesh until the potentials computed at the next inner tier of points satisfy the conditon:

$$\hat{\Phi}_{\substack{\text{induced}\\\text{extra}}}\Big|_{\substack{\text{next inner}\\\text{tier}}} < 0.01\ \hat{\Phi}_{\text{applied}}\Big|_{\substack{\text{next inner}\\\text{tier}}}, \tag{15}$$

where the requirement of an induced potential less than 1 % of the applied potential has been found to be a sufficiently stringent condition for accurate potential calculations (see Accuracy).

In practice, this procedure for the condition at infinity (equations 14 and 15) is easily implemented and the potentials calculated at points not involved with the condition at infinity are found to be relatively insensitive to adjustments made in the mesh spacing and/or the number of mesh points.

SUCCESSIVE OVERRELAXATION

Having obtained the necessary finite difference equations for the calculations of biopotentials (equations 3, 4, 11–15), we must now find the set of potential values which will simultaneously satisfy all of these equations. A suitable technique for finding these values is the method of successive overrelaxation, which, when applied to the above finite difference equations, satisfies the necessary criteria of being both accurate and rapidly convergent.

In outline, the method of successive overrelaxation consists of three steps; first, an initial guess is made, from physical considerations, for the value of the potential at each mesh point; then, repetitive passes are made through the mesh, calculating new values for the potential at each point; finally, the process is terminated when the change in potential values per iteration becomes sufficiently small. At each pass the new value of potential at any point is obtained from the following replacement

equation:

$$\hat{\Phi}_0 = \hat{\Phi}_0 + \Omega \times (\hat{\Phi}_0^* - \hat{\Phi}_0),$$

where the value of $\hat{\Phi}_0$ is replaced by the expression on the right and where the value of $\hat{\Phi}_0^*$ is obtained by using the appropriate finite difference equation for point 0 (equation 3, 4, 11, 12, 13, or 14). The use of a replacement equation results in "successive" updating of the values of potential as one proceeds through the mesh. The "overrelaxation" constant Ω is used to accelerate the convergence of the technique by increasing the change in potential values per iteration ($\Omega \geq 1$).

With this overview in mind, we can now proceed to examine the convergence and accuracy properties of the finite difference-successive overrelaxation technique as determined by calculating the biopotentials within and surrounding a spheroidal cell in an applied uniform field parallel to the cell's axis of symmetry. As pointed out in the introduction, the midplane symmetry of this problem allows one to place mesh points in only one rather than two quadrants of a plane which contains the axis of symmetry. In order to use this reduced number of mesh points, however, an additional finite difference equation must be developed for the value of potential at the intracellular membrane point just above the midplane. Setting the value of potential along the midplane equal to zero, we can rewrite equation 11 for this point as follows, with $\hat{\Phi}_{\substack{\text{induced} \\ \text{intra(1)}}} = 0$ and by symmetry $\hat{\Phi}_{\substack{\text{induced} \\ \text{intra(2)}}} = -\hat{\Phi}_{\substack{\text{induced} \\ \text{intra(0)}}}$ (see Fig. 3):

$$\hat{\Phi}_{\substack{\text{induced} \\ \text{intra(0)}}} = \{\hat{\Phi}_{\substack{\text{induced} \\ \text{extra(0)}}} - (\sigma_{\text{intra}}/\hat{Y}_{\text{memb}})\,(-\hat{E}_{\substack{\text{applied} \\ \text{normal}}}\Big|_0 + \sum_{i=3}^{4} a_{\text{intra}(i)}\hat{\Phi}_{\substack{\text{induced} \\ \text{intra}(i)}})\}/\{1 + (\sigma_{\text{intra}}/\hat{Y}_{\text{memb}})(a_{\text{intra(0)}} - a_{\text{intra(2)}})\}.$$

The physical parameters chosen for the accuracy and convergence calculations were as follows: $\sigma_{\text{intra}} = \sigma_{\text{extra}} = 0.02$ mho/cm, $\sigma_{\text{memb}} = 0.0003$ mho/cm^2, $C_{\text{memb}} = 1\ \mu$F/cm^2, $|\hat{E}_{\text{applied}}| = 10$ v/cm, and $\omega = 300$ rad/sec. This combination of membrane parameters and angular frequency results in equal real and imaginary parts for the complex membrane admittance ($\hat{Y}_{\text{memb}} = 4.24 \times 10^{-4} e^{45°j}$ mho/cm^2).

Accuracy

The accuracy of the finite difference-successive overrelaxation technique was tested on the problem of a spherical cell in a uniform applied field. A closed form analytic solution for this problem is given below and a comparison was made between the numerical and analytic solutions at each mesh point:

$$\hat{\Phi}(z)_{\substack{\text{total} \\ \text{intra}}} = [1 - 2\sigma/(2\sigma + 3R\hat{Y}_{\text{memb}})]\hat{\Phi}(z)_{\text{applied}},$$

$$\hat{\Phi}(\rho, z)_{\substack{\text{total} \\ \text{extra}}} = \{1 + (1/r^3)[\sigma R^3/(2\sigma + 3R\hat{Y}_{\text{memb}})]\}\hat{\Phi}(z)_{\text{applied}},$$

where $r = \sqrt{\rho^2 + z^2}$, $\sigma = \sigma_{\text{intra}} = \sigma_{\text{extra}}$, $\hat{\Phi}(z)_{\text{applied}} = -z\hat{E}_{\text{applied}}$ is the applied uniform field, and R is the radius of the cell. An equipotential plot and a relative

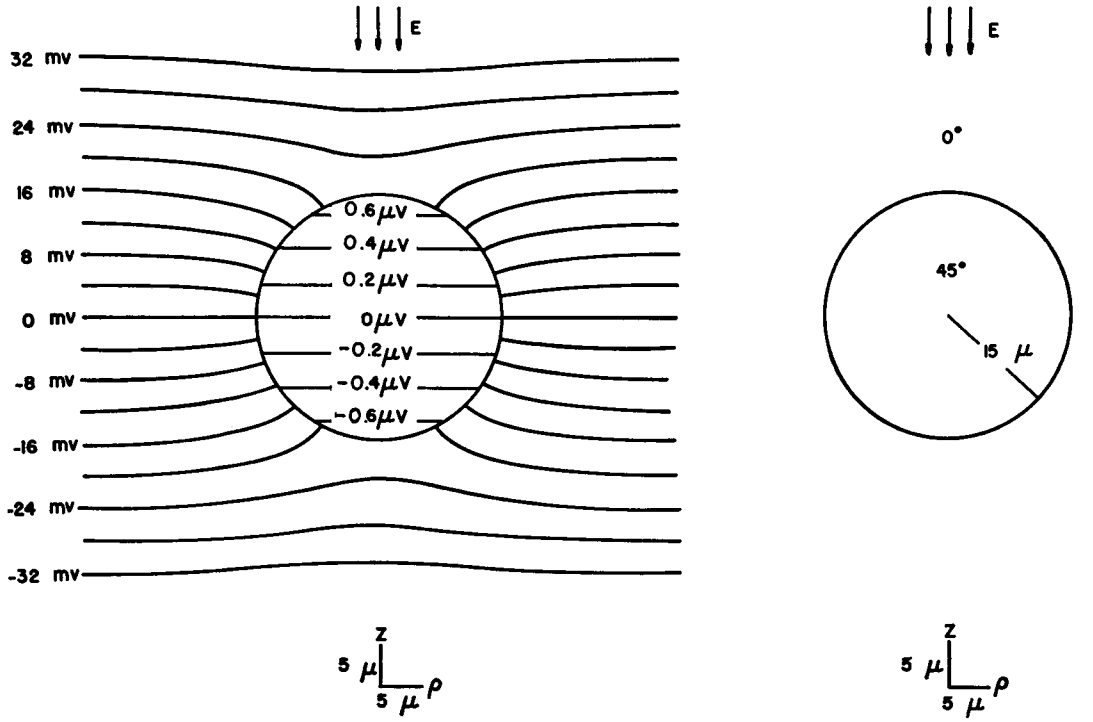

FIGURE 4 Equipotential and relative phase plot for a spherical cell in an applied uniform field. Physical parameters: $|\hat{E}_{applied}| = 10$ v/cm, $\omega = 300$ rad/sec, $\sigma_{memb} = 0.0003$ mho/cm², $C_{memb} = 1$ μF/cm², $\hat{Y}_{memb} = 4.24 \times 10^{-4} e^{45°i}$ mho/cm², $\sigma_{intra} = \sigma_{extra} = 0.02$ mho/cm, $R = 15$ μ. Note: different intra- and extracellular voltage scales; essentially normal intersection of extracellular equipotential lines and the cell membrane; agreement between the phases of the uniform intracellular field and the membrane admittance.

phase plot are shown in Fig. 4, where the radius of the cell has been chosen to be 15 μ.

For the mesh shown in Fig. 1 *a*, the average error between the numerical and analytic solutions for the magnitude of complex total potential was 1.2% extracellularly and 1.3% intracellularly, the maximum errors being 5.0% extracellularly and 3.2% intracellularly. In the calculations of phase, the agreement between numerical and analytic solutions was within 5×10^{-3} rad at all mesh points.

With finer meshes, such as that of Fig. 1 *b*, similar small errors were obtained. In general, the values of potential calculated by the numerical technique and thus, the errors, appear insensitive to the exact number and details of arrangement of the mesh points provided a sufficiently fine mesh has been employed.

Convergence

The finite difference-successive overrelaxation technique was found to be rapidly convergent for a wide range of spheroidal cells. The rate of convergence was a

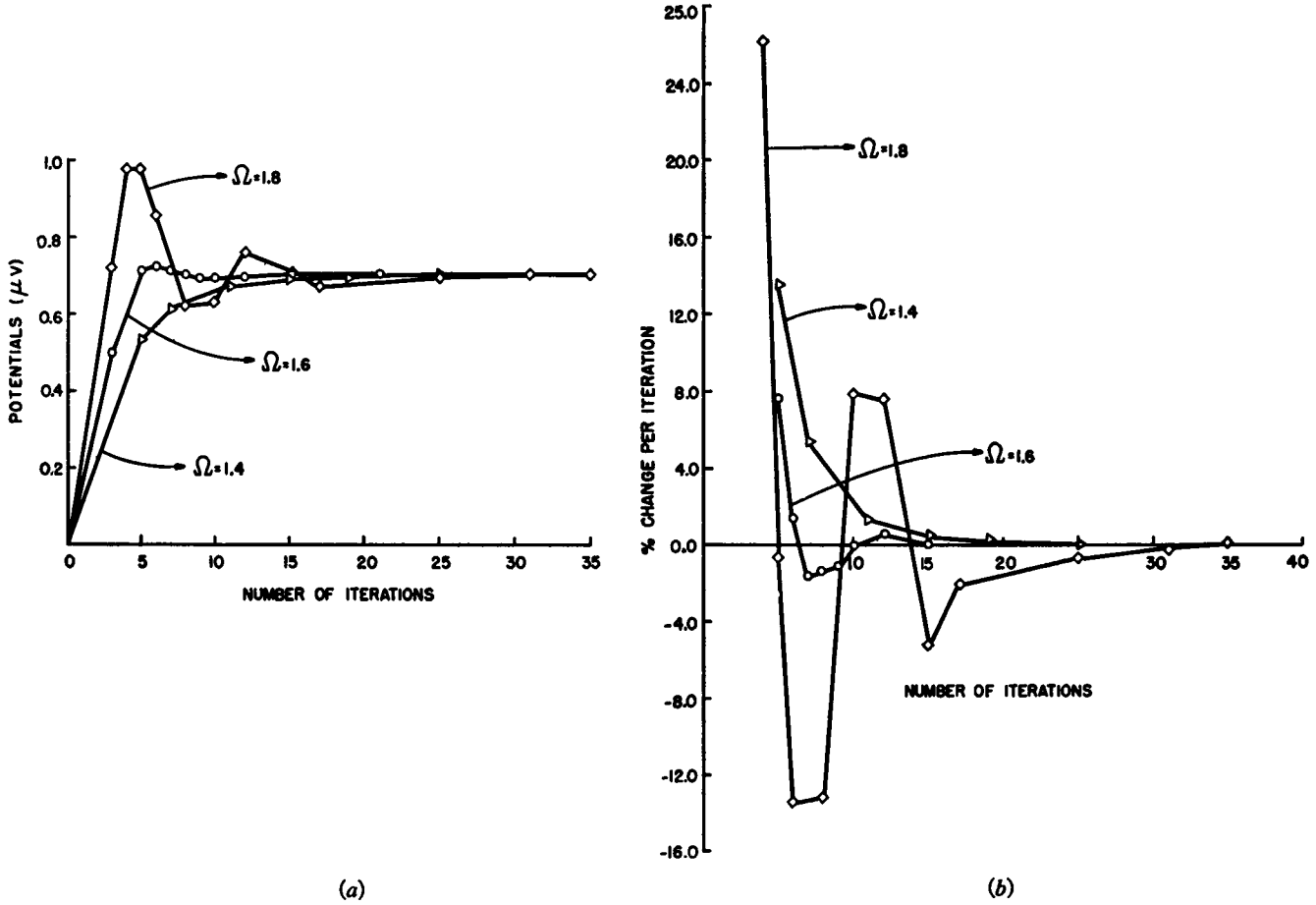

(*a*) (*b*)

FIGURE 5 Convergence as a function of overrelaxation constant Ω. (*a*) Potential vs. number of iterations. (*b*) Percentage change per iteration vs. number of iterations. Ω = 1.4, 1.6, 1.8. Data for point indicated by arrow in Fig. 1 *a*.

function of the value of the overrelaxation constant, the total number of mesh points and the arrangement of the mesh points.

Results are presented below for a spherical cell having a 15 μ radius and for a prolate spheroidal-shaped cell having a major axis of 15 μ and a minor axis of 1.5 μ. In all cases the phase converged before the magnitude of complex potential and thus only the latter will be discussed. Within a given mesh, different rates of convergence could be found as a function of point location and initial guess, which, in view of the uniform field stimulation, was taken as the total field equal to the applied field, extracellularly, and the total field equal to zero, intracellularly. The data discussed below represents the behavior of the magnitude of complex total potential of a typical slowly converging point within the mesh under consideration.

The dependence on the value of Ω is shown in Fig. 5 *a*, where the magnitude of complex total potential, at the point indicated by an arrow in the mesh plot of Fig. 1 *a*, is plotted vs. the number of iterations for three values of the overrelaxation constant Ω. In Fig. 5 *b* is plotted the more sensitive convergence measure of per-

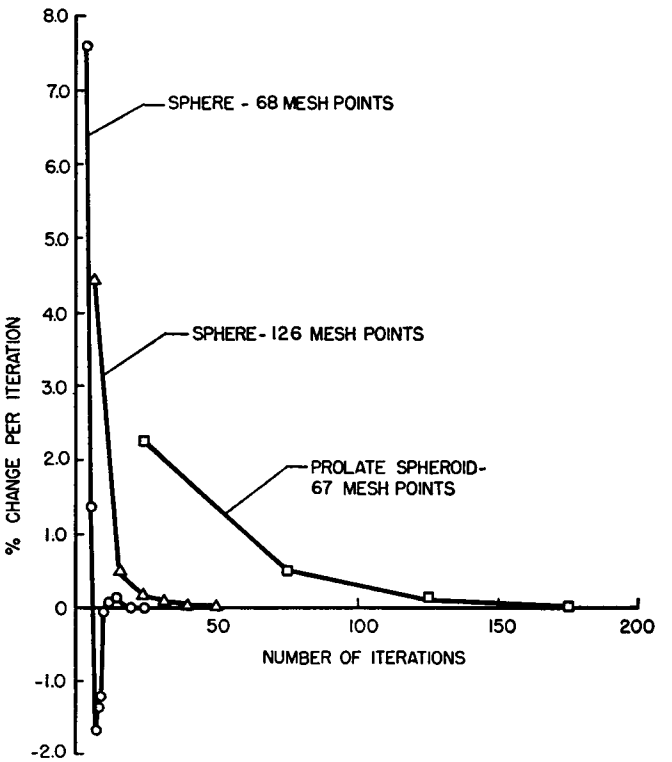

FIGURE 6 Convergence as a function of number of mesh points and arrangement of mesh points. Percentage change per iteration vs. number of iterations for points indicated by arrows in Figs. 1 *a*, *b*, *c*. $\Omega = 1.6$.

centage change per iteration, defined as:

$$\text{per cent change per iteration} = \frac{|\hat{\Phi}_{\text{total}}^{(n)}| - |\hat{\Phi}_{\text{total}}^{(n-1)}|}{|\hat{\Phi}_{\text{total}}^{(n)}|} \times 100,$$

where n is the number of iterations. As can be seen, a near optimum rate of convergence is obtained for $\Omega = 1.6$, with slower convergence occurring for $\Omega = 1.4$, and highly oscillatory, slower convergence with $\Omega = 1.8$. For even larger values of Ω (1.9), the solution becomes unstable and does not converge. In general, the value of the optimum overrelaxation constant is a function of both the number of mesh points and the arrangement of the mesh points, and, for biological problems, can only be found by trial and error.

The dependence of convergence rate upon the number and the arrangement of the mesh points is shown in Fig. 6 where the percentage changes per iteration of the magnitudes of complex total potential are plotted vs. the number of iterations for the points indicated by arrows in Figs. 1 *a*, *b*, and *c*. The value of the overrelaxation constant was taken as 1.6 for all these calculations. As can be seen, an increased number of mesh points leads to a somewhat slower rate of convergence, while a rearrangement of a given number of mesh points into a mesh having highly disparate mesh spacings (the prolate spheroid) greatly reduces the rate of convergence.

From a practical point of view, the reduced rate of convergence seen with a nonoptimum overrelaxation constant, an increase in the number of mesh points, or a rearrangement of mesh points will not be a serious problem for most physiological situations, since all of the convergence rates shown can be characterized as rapid.

SUMMARY

In summary, the finite difference equations necessary for calculating the three-dimensional, time-varying biopotentials of axially symmetric cells have been presented. The method of successive overrelaxation was employed to solve these equations and was shown to be rapidly convergent and accurate for the exemplary problem of a spheroidal cell under uniform field stimulation.

We would like to thank Dr. Gerald Hedstrom of the Department of Mathematics, Case Western Reserve University, for his guidance and encouragement of this research.

This research was supported by the U. S. Public Health Service through grants GM 1090, HE 10417, and 5 F01 GM 42313-03, from the National Institutes of Health.

Received for publication 27 August 1971.

REFERENCES

CLARK, J., and R. PLONSEY. 1968. The extracellular potential field of the single active nerve fiber in a volume conductor. *Biophys. J.* 8:842.

EISENBERG, R. S., and E. ENGLE. 1970. The spatial variation of membrane potential near a small source of current in a spherical cell. *J. Gen. Physiol.* **55**:736.

EISENBERG, R. S., and E. A. JOHNSON. 1970. Three-dimensional electrical field problems in physiology. *Progr. Biophys. Mol. Biol.* **20**:1.

FORSYTHE, G. E., and W. R. WASOW. 1960. Finite-Difference Methods for Partial Differential Equations. John Wiley and Sons, Inc., New York.

GREENSPAN, D. 1965. Introductory Numerical Analysis of Elliptic Boundary Value Problems. Harper & Row, Publishers, New York.

HELLERSTEIN, D. 1968. Passive membrane potentials. *Biophys. J.* **8**:358.

ISAACSON, E., and H. B. KELLER. 1966. Analysis of Numerical Methods. John Wiley and Sons, Inc., New York.

KINNEN, E., and D. NEWTON. 1966. Iterative Computer Solutions to Laplace's Equations in Two and Three Dimensions. University of Rochester College of Engineering and Applied Science, Department of Electrical Engineering Report.

LORENTE DE NÓ, R. 1947. A study of nerve physiology. The Rockefeller Institute Studies. New York. **132**:384.

PLONSEY, R. 1969. Bioelectric Phenomena. McGraw-Hill Book Company, New York.

PLONSEY, R., and D. B. HEPPNER. 1967. Considerations of quasi-stationarity in electrophysiological systems. *Bull. Math. Biophys.* **29**:657.

RALL, W. 1969. Distributions of potential in cylindrical coordinates and time constants for a membrane cylinder. *Biophys. J.* **9**:1509.

SHORTLEY, G. H., R. WELLER, P. DARBY, and E. H. GAMBLE. 1947. Numerical solution of axisymmetrical problems with applications to electrostatics and torsion. *Ohio State Univ. Eng. Exp. Sta. Bull.* **128**:1.

TERRY, F. H. 1967. Iterative solution of Neumman boundary value problem with application to electrocardiography. Ph.D. Thesis. Case Western Reserve University, Cleveland, Ohio.

VAYO, H. W. 1965. Green's function for a spherical cell. *J. Math. Anal. Appl.*, **10**:25.

WEINBERG, A. M. 1942. Green's functions in biological potential problems. *Bull. Math. Biophys.* **4**:107.